



North Equatorial Indian Ocean Convection and Indian Summer Monsoon June Progression: a Case Study of 2013 and 2014

RAMESH KUMAR YADAV¹ and BHUPENDRA BAHADUR SINGH¹

Abstract—The consecutive summer monsoons of 2013 and 2014 over the Indian subcontinent saw very contrasting onsets and progressions during the initial month. While the 2013 monsoon saw the timely onset and one of the fastest progressions during the recent decades, 2014 had a delayed onset and a slower progression phase. The monthly rainfall of June 2013 was +34 %, whereas in 2014 it was –43 % of its long-period average. The progress/onset of monsoon in June is influenced by large-scale circulation and local feedback processes. But, in 2013 (2014), one of the main reasons for the timely onset and fastest progression (delayed onset and slower progression) was the persistent strong (weak) convection over the north equatorial Indian Ocean during May. This resulted in a strong (weak) Hadley circulation with strong (weak) ascent and descent over the north equatorial Indian Ocean and the South Indian Ocean, respectively. The strong (weak) descent over the south Indian Ocean intensified (weakened) the Mascarene High, which in turn strengthened (weakened) the cross-equatorial flow and hence the monsoonal circulation.

Key words: ISM, Mascarene High, Hadley circulation, OLR, Cross-equatorial flow, ENSO.

1. Introduction

Rainfall over the Indian subcontinent has a unique annual cycle where more than 80 % of the annual precipitation occurs during a short span of 4 months, which commences in the month of early June and continues till September end, most commonly termed as Indian summer monsoon (ISM) rainfall. ISM, which is a part of the Asian monsoon system, has significant temporal and spatial variations. ISM generally has its onset over the southwest coast around 1 June with a standard deviation of about 8 days, and progresses northward to cover the entire country by

15 July (Pai and Rajeevan 2009). The onset of ISM is the most anxiously awaited weather singularity in the Indian subcontinent as it heralds the rainy season and marks the end of the hot summer. The onset and progression of ISM is represented by the abrupt transition from dry to wet conditions, starting at the southwest coast of India before rapidly blanketing most of the rest of the country (Lau and Yang 1996; Wu and Wang 2001). The onset and progression of ISM have a pronounced interannual variability (Joseph et al. 1994; Wang and LinHo 2002; Gadgil 2003; Li and Zhang 2009) that is partly inherited from large-scale circulation and thermodynamic features. Researchers have tried to explain the onset and progression of ISM by several theories, e.g., land–ocean heat contrast, shifting of the inter-tropical convergence zone due to the effect of varying solar insolation, jet stream theory, etc. Apart from that, there are remote factors (e.g., El Nino, La Nina) that have a profound effect on the ISM (Sikka 1980; Angell 1981; Ropelewski and Halpert 1987, 1989; Rasmusson and Carpenter 1983; Shukla 1987; Yadav 2009a, b).

The ISMs of 2013 and 2014 were quite distinct, especially in their onset as well as in initial progression phase during the early monsoon month of June. The year 2013 witnessed the fastest advancement of ISM in the last 70 years (IMD 2013). The monsoon covered the entire country in just 16 days after its onset over the southwest coast on 01 June, i.e., by 16 June, which is almost a month ahead of its climatological date. June 2013 was exceptional due to its strong, timely onset and rapid progression phase. The rainfall over the country during June 2013 was 134 % of its long-term mean (IMD 2013). On the other hand, the 2014 monsoon had a delayed onset on

¹ Indian Institute of Tropical Meteorology, Pashan, Pune 411 008, India. E-mail: yadav@tropmet.res.in

06 June, exhibited a sluggish northward progression and covered the whole country by 17 July. During most of June 2014, the rainfall was almost absent over central India. The rainfall over the country during June 2014 was only 56.5 % (source: http://www.imdpune.gov.in/mons_monitor/mm_index.html).

In this study, we have focused on 2013 and 2014 in particular, as none of these 2 years exhibited any strong El Nino or La Nina type of conditions. Though the boreal summer of 2014 initially had the signals of El Nino, it weakened further. In 2014, the cumulative rainfall prior to August was less than the normal. Later in the months of August and September 2014 the ISM recovered, but the initial deficiency during the onset month led to the seasonal rainfall being less than the normal. Hence in particular, the analysis is centered on the early phase of the monsoon. To check the robustness of the feature, we look for other years as well, omitting the strong cases of El Nino or La Nina events. Of course, the conditions which build up over the Indian Subcontinent and around have an established relationship with the seasonal (June–September) rainfall, but the strong cross-equatorial flow of moisture-laden winds is directly influenced by the presence of sustained high pressure over the mid-latitudes in the south Indian Ocean. A buildup of relatively high pressure prior to the month of June, we argue, may lead to the timely onset and supply the initial momentum for faster progression.

2. Data and Methodology

The global atmospheric reanalysis dataset ERA-Interim has been used in this study. ERA-Interim is the latest European Centre for Medium-Range Weather Forecasts (ECMWF) global atmospheric reanalysis of the period 1979 to the present. ERA-Interim was originally planned as an ‘interim’ reanalysis in preparation for the next-generation extended reanalysis to replace ERA-40. It uses a December 2006 version of the ECMWF Integrated Forecast Model (IFS Cy31r2). It originally covered dates from 1 January 1989, but an additional decade, from 1 January 1979, was added later. ERA-Interim is being continued in real time. The spectral resolution is T255 (about 80 km) and there are 60

vertical levels, with the model top at 0.1 hPa (about 64 km). The data assimilation is based on a 12-h four-dimensional variational analysis (4D-Var) with adaptive estimation of biases in satellite radiance data (VarBC). With some exceptions, ERA-Interim uses input observations prepared for ERA-40 until 2002, and data from ECMWF’s operational archive thereafter (Dee et al. 2011). Daily and monthly outgoing longwave radiation (OLR) data at 2.5° latitude \times 2.5° longitude grid provided by the NOAA/OAR/ESRL PSD, Boulder, USA, from the website <http://www.esrl.noaa.gov/psd/> have been used (Liebmann and Smith 1996). Daily and monthly means of different atmospheric fields for the months of May and June have been analyzed to find out the underlying mechanisms for the onset and progression of ISM in the two contrasting consecutive years of 2013 and 2014. The simultaneous correlation coefficient of negative Nino-3 index with sea surface temperature (SST) and 200-hPa velocity potential have been calculated to study the influence of ENSO on SST and Walker circulation. Nino-3 index is obtained by extracting SST data from the box 5°N – 5°S and 150°W – 90°W . The velocity potential is calculated from the zonal and meridional wind component.

3. Results

The years 2013 and 2014 were two consecutive contrasting ISM years with respect to their onset and progression in the month of June. In 2013, the onset was timely (01 June) and the progression was very fast, while in 2014, the onset was delayed (06 June) and the progression was very lethargic. The cumulative rainfall of 2013 June was +34 %, whereas 2014 June recorded –43 % of its long-period average. Therefore, the spatial plots of monthly means for the month of May 2013 and 2014 and their difference in atmospheric parameters are expected to provide further insight into the changes observed in the succeeding months of June. Figure 1 shows the OLR (gray shaded), mean sea level pressure (MSLP; contours) and 850-hPa wind (black arrows) for the month of May 2013 (Fig. 1a), 2014 (Fig. 1b) and the difference of 2013 and 2014

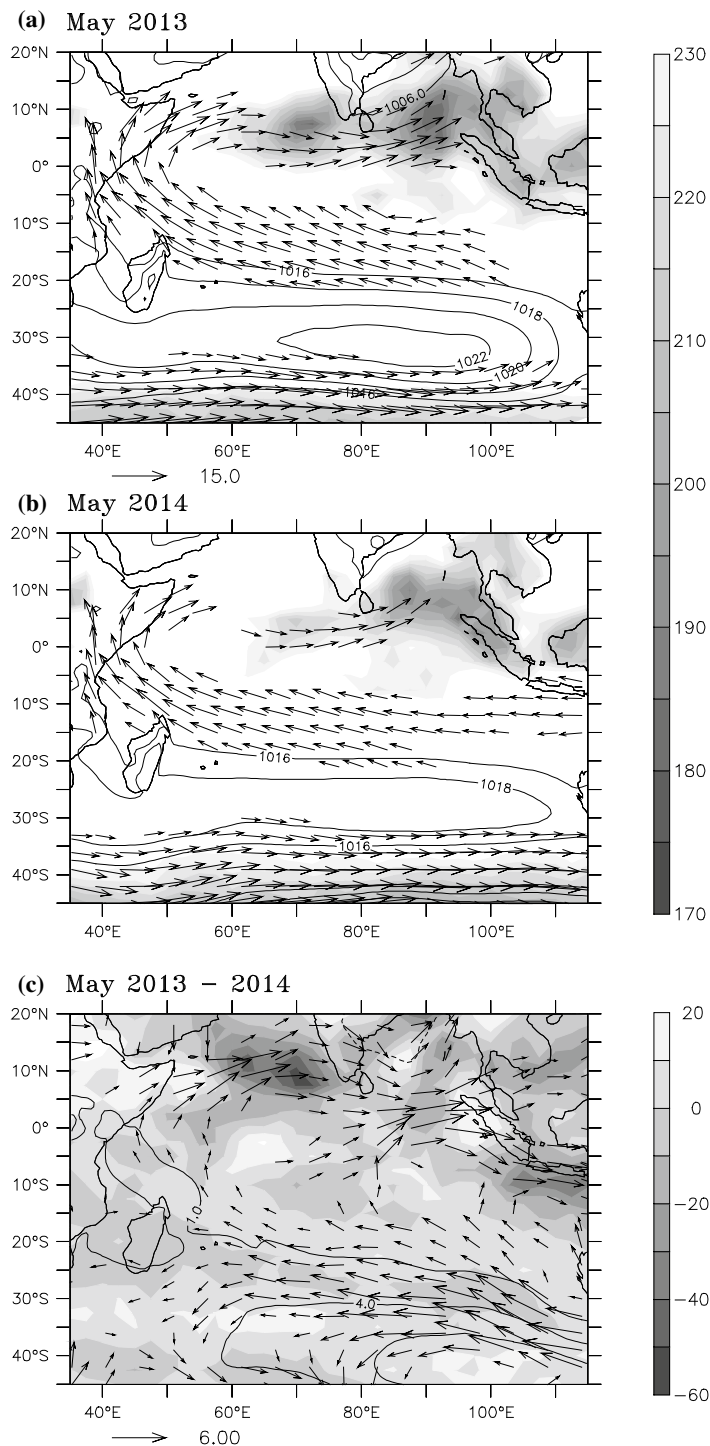


Figure 1

MSLP (contours, hPa), 850 hPa winds (vectors, ms^{-1}), OLR (gray shaded, Wm^{-2}). **a** May 2013 and **b** May 2014. **c** Difference in May 2013 and May 2014 MSLP (contours), OLR (gray shaded) and 850-hPa wind (vectors)

(Fig. 1c). The MSLP over Mascarene High was more intense in 2013 than 2014 (Fig. 1a, b). It caused the buildup of higher north–south (N–S) pressure gradient, resulting in stronger cross-equatorial flow in 2013 as compared to 2014. Since OLR is a good proxy for deep convection: in Fig. 1a, b, low OLR values, less than 220 W/m^2 , indicate deep convection and pronounced condensational heating over the tropical and subtropical regions (Liebmann and Smith 1996). As compared to 2013, where the deep convection over the equatorial north Indian Ocean was much wider, during 2014 it was concentrated toward east and deep convection over the north equatorial Indian Ocean was relatively less intense. The difference plot of OLR and 850-hPa wind between 2013 and 2014 (Fig. 1c) shows deep convection over the south Arabian Sea and intense cross-equatorial flow in 2013 as compared to 2014.

Similarly, Fig. 2 shows the SST (color shaded) and 200-hPa velocity potential (contours) for the month of May. The SST was warmer than 28°C in the tropical Indian and the western Pacific during both years. The velocity potential shows tripole type of structure over the tropical Indo-Pacific Ocean with upper-level divergence (velocity potential minimum) over the warm pool region of Indonesia and the western Pacific and convergence (velocity potential maximum) over the western Indian Ocean and the eastern Pacific. This structure represents the Walker circulation with upper-level divergence and convergence over the warm pool region and the eastern Pacific, respectively. In 2013, the Walker circulation was much stronger than in 2014. The difference between the 2013 and 2014 May month shows cooler SST anomaly all along the equatorial Indo-Pacific Ocean, except the warm pool region. The difference pattern resembles the initial stage of La Nina conditions because 2014 had minor signatures of El Nino during the month which weakened afterward. The difference in SST over the tropical India Ocean was very marginal. This suggests that the tropical Indian Ocean SST was not substantially influential in modulating the deep convection as observed during the mentioned years. The velocity potential shows divergence anomaly all along the tropical Indo-Pacific Ocean except the western Indian Ocean and the eastern Pacific.

To study the upper-level horizontal temperature gradient, the sub-tropical westerly jet stream and tropical easterly jet stream for the month of May during 2013 and 2014, the 200-hPa level temperature (color shaded) and zonal wind (contours) have been plotted in Fig. 3. The horizontal temperature gradient between the northern India and the equatorial Indian Ocean was greater in 2013 than 2014. The sub-tropical westerly jet stream over the north of India and the tropical easterly jet stream over the equatorial Indian Ocean were more intense in 2013 than 2014 (Fig. 3c). This suggests that the deep convection over the north Indian Ocean during May 2013 had intensified the upper-level divergence which is directly correlated with anti-cyclonic circulation. The anti-cyclonic circulation intensified both the sub-tropical westerly jet toward the north of India and the tropical easterly jet stream at the equatorial Indian Ocean. The strong sub-tropical westerly jet stream advected the temperatures to the northern India (Fig. 3a).

Figure 4 shows the Hadley circulation averaged between the longitudes 60°E and 90°E for May 2013 (upper panel), 2014 (middle panel) and the difference between 2013 and 2014 (lower panel). In 2013, the Hadley circulation was more intense than in 2014 (Fig. 4a, b). The difference plot (Fig. 4c) suggests that there was a slightly northward shift in the ascent and descent of the Hadley circulation in 2013 when compared with 2014. In 2013, the ascent and descent were observed around 10°N and 20°S , respectively, whereas in 2014, the ascent and descent were confined to the equator and 25°S , respectively. The strong subsidence over the south Indian Ocean during 2013 was one of the main reasons for the intensification of Mascarene High. The stronger Mascarene High intensified the cross-equatorial monsoonal flow in 2013 and vice versa for 2014 (Krishnamurti and Bhalme 1976). The difference between the wind speed at 850 hPa (Fig. 1) is the confirmation for the same.

It is well known that the onset and progression of ISM are also affected by the northward-propagating intraseasonal variations (ISVs) by transporting moisture and momentum from tropical Indian Ocean to the Indian subcontinent (Zhou and Murtugudde 2014). Therefore, to see the northward propagation of ISVs during 2013 and 2014, we plotted the time–

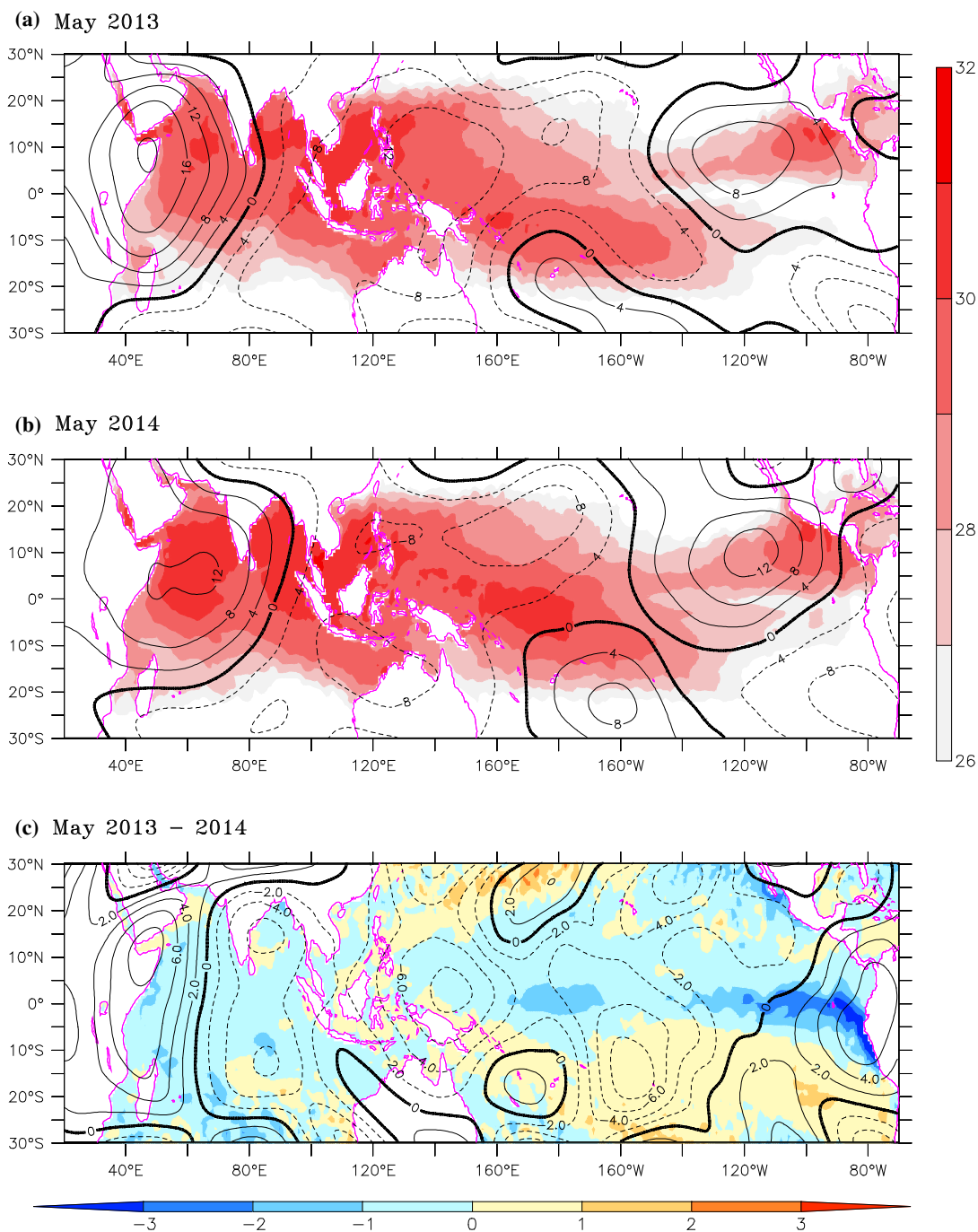


Figure 2
SST (color shaded, °C), 200-hPa velocity potential (contours, $10^6 \text{m}^2 \text{s}^{-1}$). **a** May 2013 and **b** May 2014. **c** Difference in May 2013 and May 2014

latitude cross section of OLR averaged over the longitudes 60°E–90°E from 01 May to 15 June for 2013 (Fig. 5a) and 2014 (Fig. 5b). It is seen that the

persistent deep convection up to mid-May and last week of May were stagnant over north of the equator, with no northward propagation observed in 2013. In

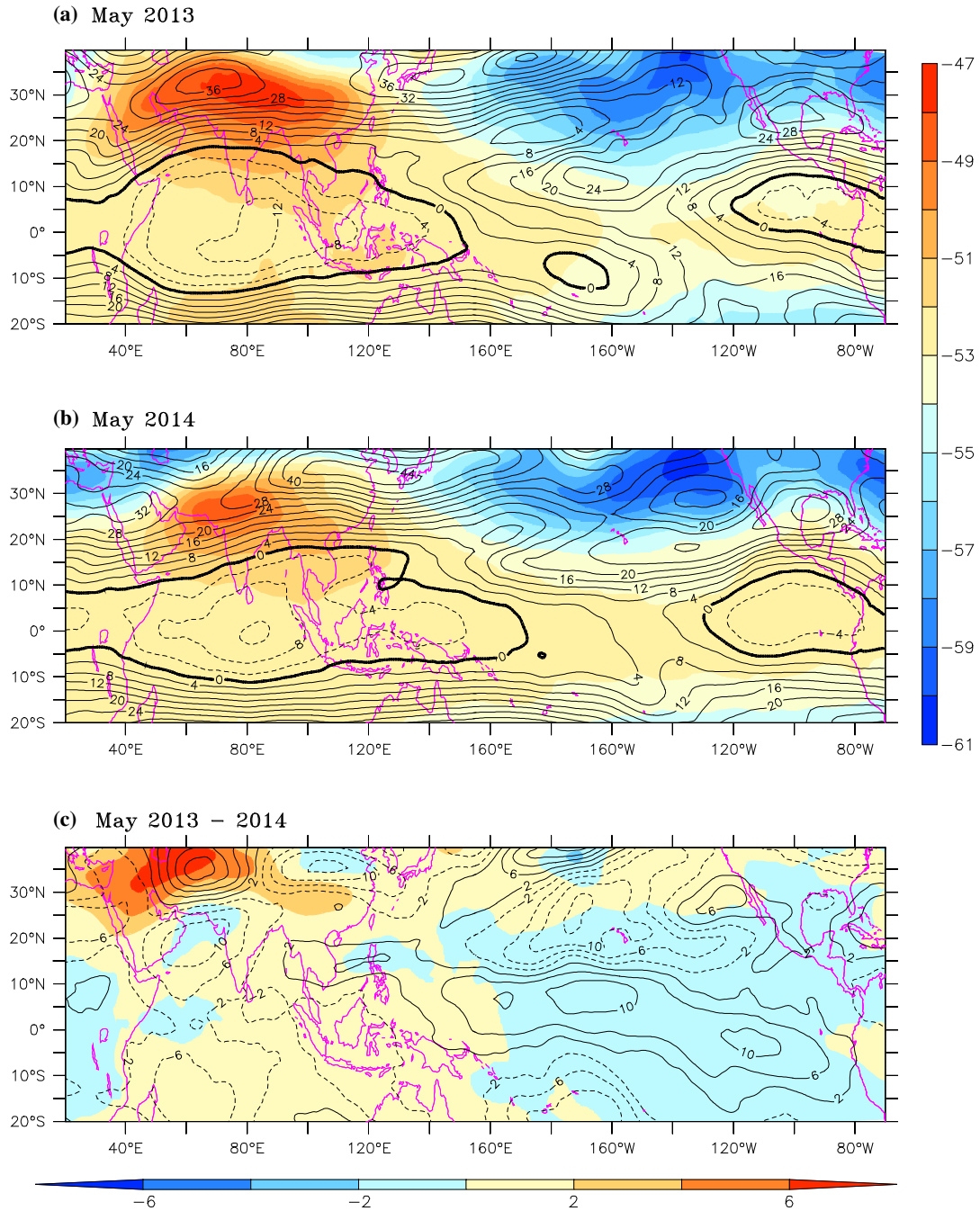


Figure 3

200-hPa temperature (color shaded, $^{\circ}\text{C}$) and zonal wind (contours, ms^{-1}). **a** May 2013 and **b** May 2014. **c** Difference in May 2013 and May 2014

the third week of May 2013, tropical deep convection was absent, while in 2014 persistent deep and northward propagation of convection was missing in

May. Similarly, we have plotted time–longitude cross section of OLR, averaged over the latitudes 10°S–10°N from 01 May to 15 June to see the eastward

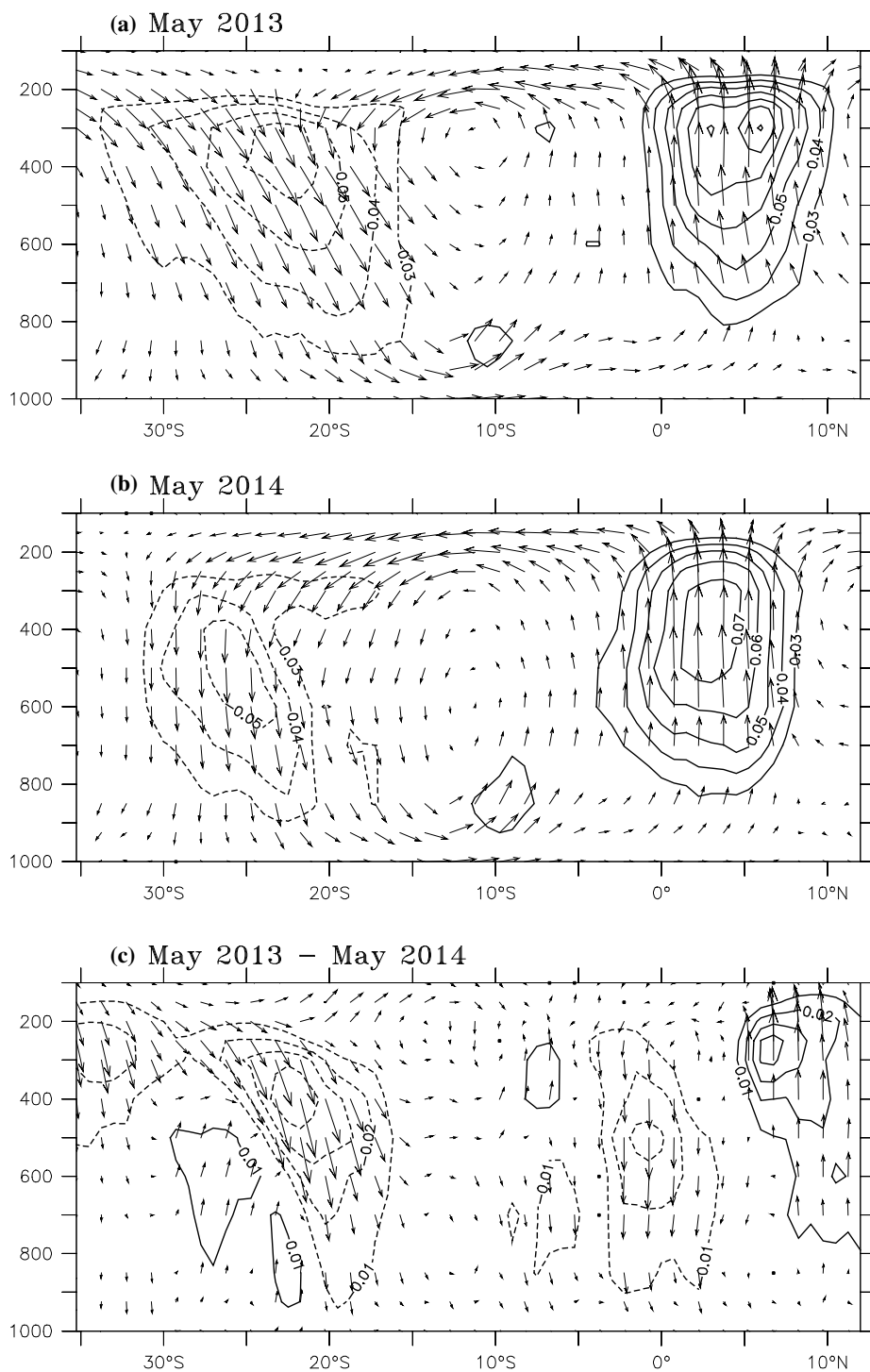


Figure 4

May Hadley circulation, representing the latitude–height section (longitude averaged from 60°E to 90°E) of meridional and pressure vertical velocities for **a** 2013 and **b** 2014 (vertical velocity scaled by 100) and **c** 2013 minus 2014 (vertical velocity scaled by 500)

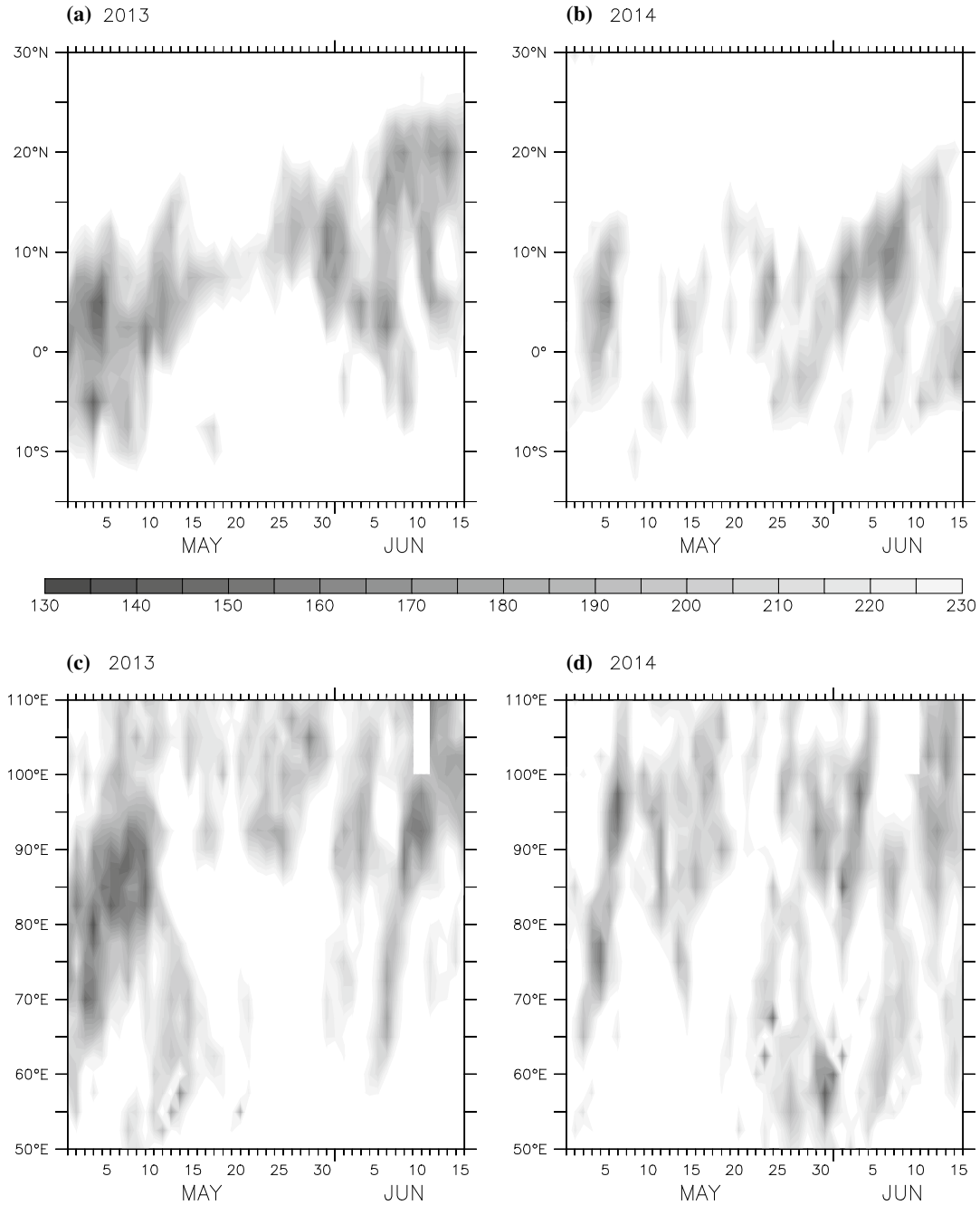


Figure 5

The time–latitude section of OLR (Wm^{-2}) along 15°S to 30°N averaged for the longitude from 60°E to 90°E for **a** 2013 and **b** 2014. The time–longitude section of OLR (Wm^{-2}) along 50°E – 110°E averaged for the latitude from 10°S to 10°N for **c** 2013 and **d** 2014. The time length is from 01 May to 15 June

propagation of ISVs in 2013 (Fig. 5c) and 2014 (Fig. 5d). The persistent deep convection observed in the first half of May 2013 shows the eastward

propagation, but for the later period of 2013 and the whole of 2014, the eastward propagation was missing. Now, it is clear that the early onset and fast

propagation of 2013 ISM was not initiated by the northward propagation of strong ISVs in that year.

From the above results, it is clear that persistent deep convection in the north equatorial Indian Ocean was one of the main reasons which led to the intensification of Mascarene High and hence the ISM circulation. Based on the observed features in Fig. 1, we extracted daily indexes for 2013 and 2014 from the area-averaged OLR in the region 60°E – 90°E and 2.5°S – 7.5°N and MSLP in the region 60°E – 90°E and 20°S – 30°S (with special emphasis on the below 220 Wm^{-2} values for OLR and above 1019 hPa for MSLP) termed hereafter as OLRIO and MH, respectively. The daily plots for May OLRIO and MH are shown in Fig. 6a, b, respectively. In 2013, well-organized deep convection was observed in the first half of May which was missing in 2014. Similarly, Mascarene High was intense between 7 and 24 May in 2013, while in 2014 it consistently lacked in intensity throughout the month. This clear distinction in the OLRIO and MH fields in the month of May was one of the important factors which modified the onset and progression of ISM in the successive years of 2013 and 2014.

To see the nature and robustness of the relationship between OLRIO and MH, we calculate the lag correlation of MH with respect to OLRIO from 01 May to 15 June for 2013 and 2014 and have been

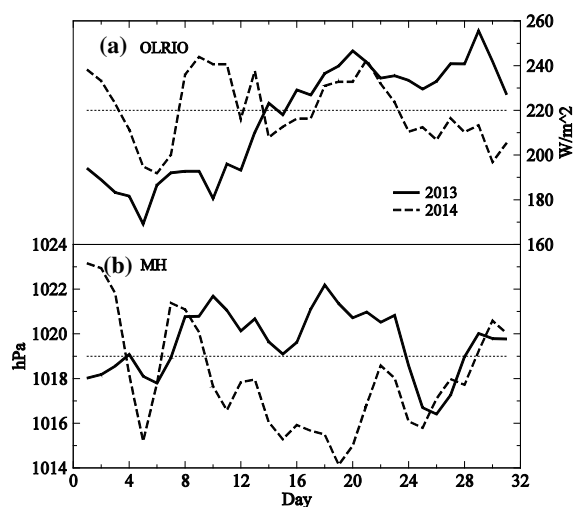


Figure 6

Daily variations of **a** OLRIO (Wm^{-2}) and **b** MH (hPa) for May 2013 and 2014

shown in Fig. 7. In 2013, it shows significantly strong 6–8 days lag correlation at 99.9 % confidence level between MH and OLRIO, which suggests that the deep convection over the north equatorial Indian Ocean had fed and enhanced the MSLP over the Mascarene High through the descent of the Hadley circulation (Fig. 4). In 2014, the lag correlation shows 3 days lead of OLRIO over MH significant at the 95 % confidence level. Since the organized persistent deep convection was missing in 2014, therefore a strong correlation in 2014 is not expected. Hence, the persistent deep convection of May 2013 intensified the Mascarene High which established a good platform with nearly half a month ahead of the commencement of ISM 2013, while the lack of persistent deep convection over the north equatorial Indian Ocean failed to intensify the Mascarene High and remained normal apart from other unfavorable conditions which delayed the onset and progression of ISM 2014.

Further, to find out similar events in the past, we constructed interannual time series for May for OLRIO and MH. The year-to-year variation in the period 1979–2013 shows (Fig. 8a) that the relationship was not persistent throughout the data period. Also the 21-year sliding correlation between the two time series shows (Fig. 8b) positive correlation before central year 1995 and negative correlation after that, suggesting that the relationship has become frequent in the recent years where the deep convection over the north equatorial Indian Ocean intensifies the surface pressure over Mascarene High. In Table 1, we selected the years with OLR values less than 220 Wm^{-2} and MSLP values greater than 1019 hPa in the same year, with their onset date over the southwest peninsular coast and the percentage departure of June rainfall in the respective years. The years with a strong El Nino and La Nina are shown in bold and bold italic, respectively. 2010, 1999 and 1988, which were strong La Nina years, shows early onsets, but the percentage departures in June were not strong. 1997 and 1982 were strong El Nino years; again, the percentage departures in June were not strong. 1997 had a delayed onset, while in 1982 the onset was early. However, during the non-ENSO years such as 1994, 1989 and 1980, the onset and June progressions match with the year 2013.

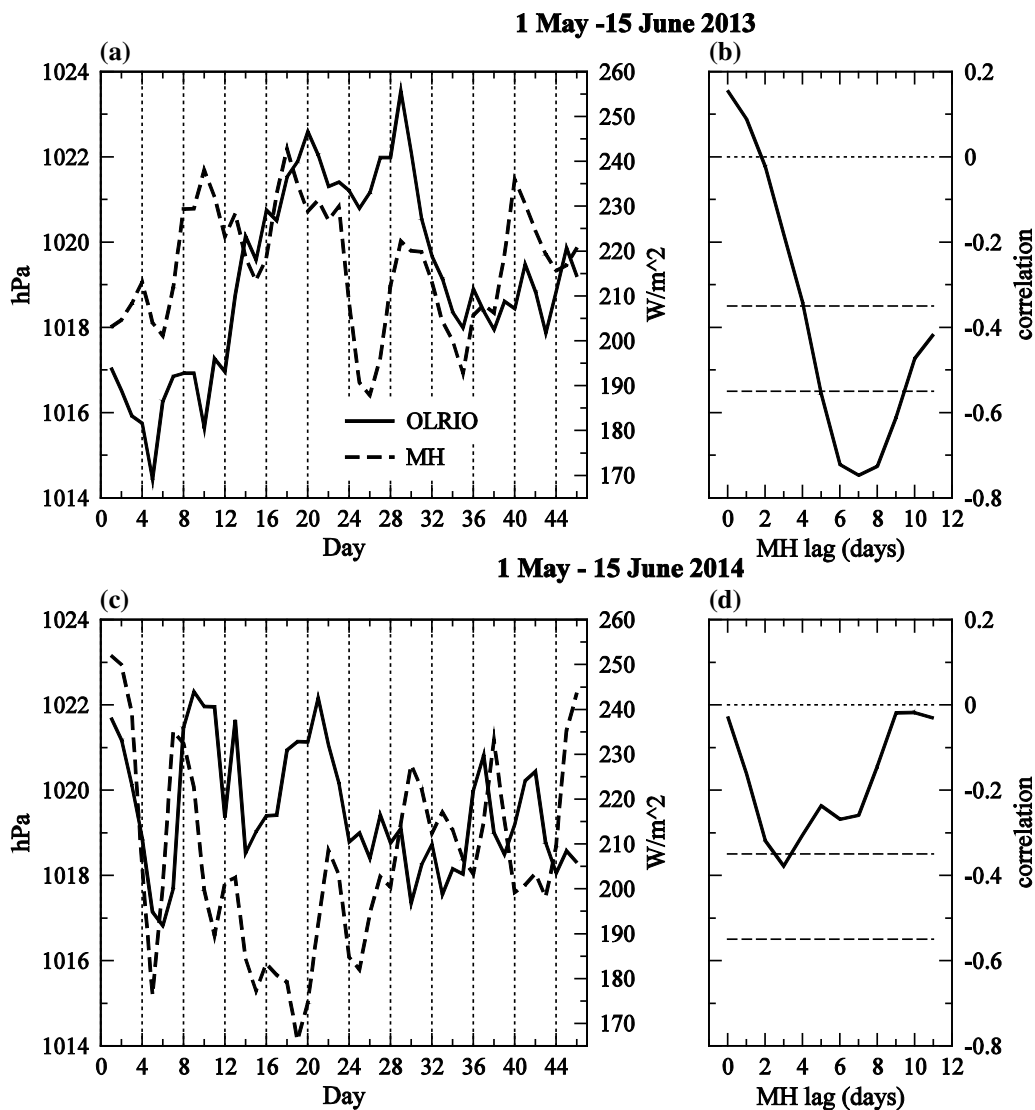


Figure 7

Daily variations of OLRIO (Wm^{-2}) and MH (hPa) from 1 May to 15 June **a** 2013 and **c** 2014. Lag correlations (*black curve*) of MH with respect to OLRIO for the period 1 May to 15 June for **b** 2013 and **d** 2014. The 95 and 99.9 % confidence levels are indicated by the *dashed black line*. The dotted line is the zero correlation line

In summary, during the non-ENSO years, the persistent deep convection during the month of May over the north Indian Ocean intensifies the local Hadley cell, which intensifies the Mascarene High. The intensified Mascarene High intensifies the cross-equatorial flow which further pushes the deep convection northward over the Indian subcontinent with abundant moisture supply. This leads to early onset and rapid progression of ISM.

4. Conclusion and Discussion

The Indian summer monsoons (ISMs) of 2013 and 2014 were contrasting in their onset and initial progression phases. In 2013, the onset was timely and the progression of ISM was the fastest in last few decades, whereas in 2014 the onset was delayed and the progression was sluggish. The June monthly rainfall in 2013 was +34 %, whereas in June 2014 it was

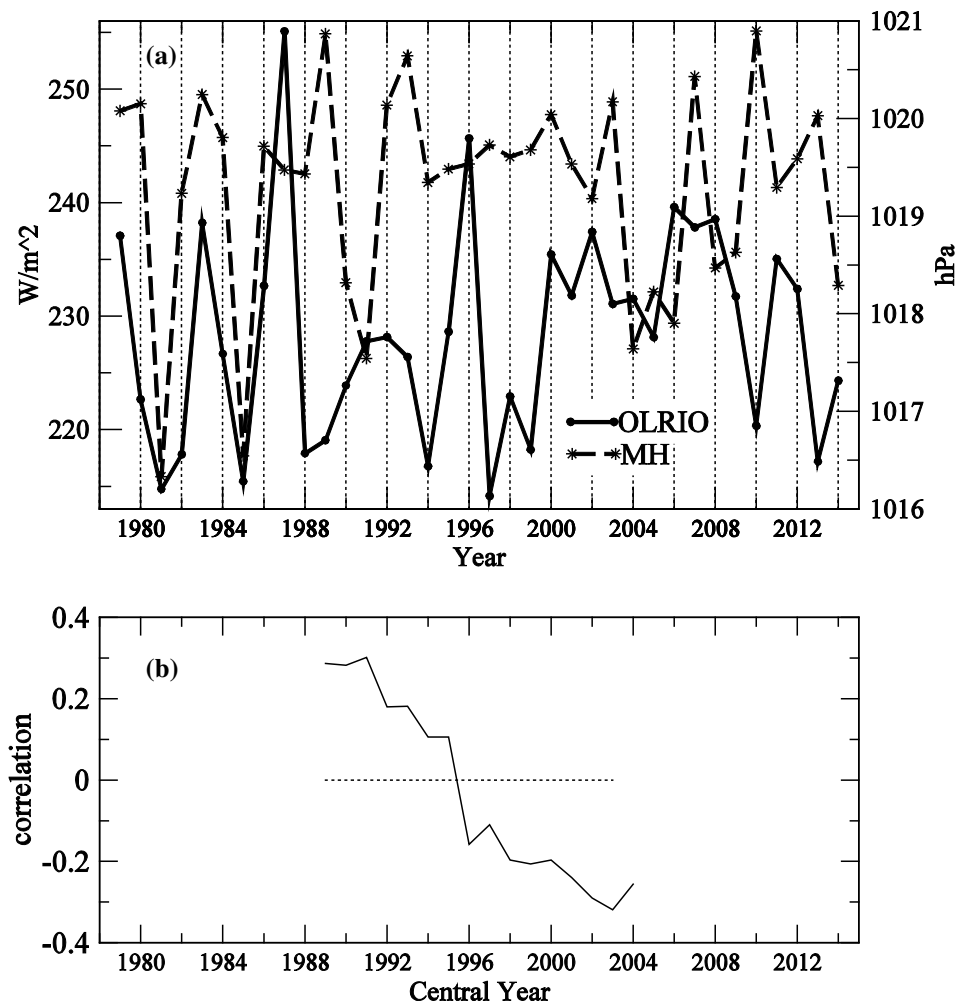


Figure 8

a Yearwise monthly variations of OLRIO and MH from 1979 to 2013. **b** Sliding correlations on a 21 year moving window between OLRIO and MH

–43 % of its long-period average. In this study, we have made an attempt to unravel the factors that generated this discrepancy in the month of June 2013 and 2014. It was found that in 2013, there was persistent deep convection in the first half of May over the north equatorial Indian Ocean, which intensified Mascarene High over the south Indian Ocean through strong Hadley circulation with strong descent over the south Indian Ocean. There was a lead of 6–8 days between deep convection over the north equatorial Indian Ocean to MSLP over the south Indian Ocean, i.e., the Hadley circulation took 6–8 days to feed the Mascarene High over the south Indian Ocean. The

intensified Mascarene High intensified the cross-equatorial flow and hence the monsoonal circulation was well established half a month ahead, which caused the timely onset and fastest progression of monsoon in the year 2013. In 2014, the persistent deep convection over the north equatorial Indian Ocean was missing, which led to weaker Hadley circulation that could not feed the Mascarene High. Therefore, the weaker Mascarene High in 2014 as compared to 2013 generated a weaker cross-equatorial flow and hence delayed onset and progression of monsoon 2014 and vice versa. This relationship is more prominent in the recent non-ENSO years.

To see the effect of ENSO on the onset and initial progression of ISM, we have considered Nino-3 index as representative of ENSO. The spatial correlation coefficient of the negative Nino-3 index on SST (color shaded) and 200-hPa velocity potential (contours) are shown in Fig. 9. The negative Nino-3 index represents La Nina conditions. The La Nina years are associated with cool SST anomaly over the equatorial Indian Ocean and warm anomaly over the

tropical north-western Pacific. The 200-hPa velocity potential shows significant negative correlation over south-east Asia and positive correlation over the equatorial central and eastern Pacific (Fig. 9). This suggests that the Walker circulation is stronger with rising motion over Cambodia and subsidence over the equatorial eastern Pacific during La Nina years and vice versa during El Nino years. The warming of the tropical north-western Pacific must have shifted and intensified the inter-tropical convergence zone to the Cambodian latitude, which in turn intensifies the Walker circulation during the La Nina years and vice versa during the El Nino years. The upper-level divergence (velocity potential minimum) anomaly over north-east and southern India (Fig. 9) reinforce the convective activity which leads to early onset of ISM during the La Nina years and vice versa for the El Nino years. In 2013, the upper-level divergence was centered over the western Pacific, whose influence on the early onset and fast progression of ISM was not so prominent. Therefore, the persistent deep convection over the north India Ocean in the month of May, like the one observed in 2013, can be a better indicator for the initial buildup of strong cross-

Table 1

Years with simultaneous OLRIO lower than 220 Wm^{-2} and MH greater than 1019 hPa

Year	Onset date	June % departure
2013	01 June	+34.5
2010	31 May	-15.6
1999	25 May	+5.1
1997	09 June	+6.4
1994	29 May	+29.0
1989	03 June	+19.3
1988	26 May	+6.8
1982	29 May	-16.8
1980	01 June	+37.7

Bold and bold italic represents the strong El Nino and strong La Nina years, respectively

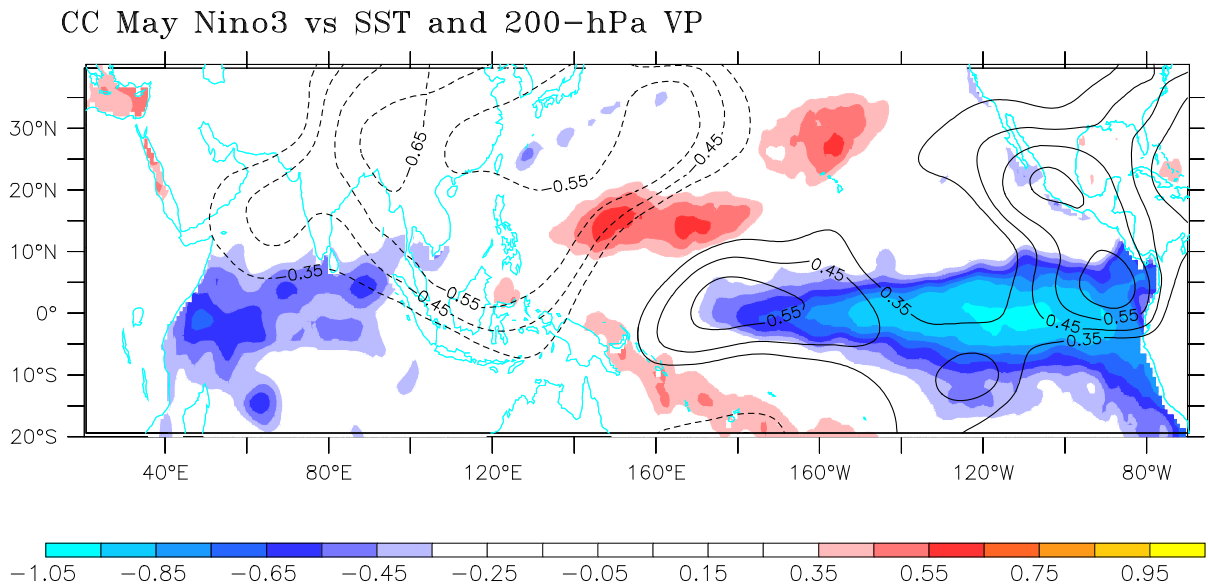


Figure 9

Spatial pattern of simultaneous correlation of May negative Nino-3 index vs SST and 200-hPa velocity potential for the period 1979–2014. SST is shown as *shaded*, and velocity potential as contours. Positive (negative) velocity potential correlations are indicated by *continuous* (*dotted*) lines. The velocity potential correlation contours start from 0.35 and the intervals are 0.1

equatorial flow leading to better forecasting of the initial ISM rainfall. This is also an important research topic which will contribute to promote progress in the science of ISM.

Acknowledgments

The authors wish to thank the editor and the two anonymous reviewers for their insightful comments that helped improve the manuscript. The data have been taken from websites and all data sources have been duly acknowledged. Computational and graphical analyses required for the study were completed with the freely available softwares, e.g., Ferret, NCL and xmgrace.

REFERENCES

- Angell, J. K. (1981). Comparison of variations in atmospheric quantities with sea surface temperature variations in the equatorial Pacific. *Monthly Weather Review*, 109, 230–243.
- Dee, D. P., et al. (2011). The ERA-Interim reanalysis: Configuration and performance of the data assimilation system. *Quarterly Journal Royal Meteorological Society*, 137(656), 553–597.
- Gadgil, S. (2003). The Indian monsoon and its variability. *Annual Review of Earth and Planetary Sciences*, 31(1), 429–467.
- IMD. (2013). Monsoon 2013: A report. IMD Met Monograph No.: ESSO/IMD/SYNOPSIS MET/01-2014/15. India Met Department Eds Pai DS and Bhan SC. <http://www.imdpune.gov.in/>.
- Joseph, P. V., Eischeid, J. K., & Pyle, R. J. (1994). Interannual variability of the onset of the Indian summer monsoon and its association with atmospheric features, El Nino, and sea surface temperature anomalies. *Journal of Climate*, 7, 81–105.
- Krishnamurti, T. N., & Bhalme, H. N. (1976). Oscillations of a monsoon system. Part I. Observational aspects. *Journal of the Atmospheric Sciences*, 33(10), 1937–1954.
- Lau, K. M., & Yang, S. (1996). Seasonal variation, abrupt transition, and intraseasonal variability associated with the Asian summer monsoon in the GLA GCM. *Journal of Climate*, 9(5), 965–985.
- Li, J., & Zhang, L. (2009). Wind onset and withdrawal of Asian summer monsoon and their simulated performance in AMIP models. *Climate Dynamics*, 32, 935–968.
- Liebmann, B., & Smith, C. A. (1996). Description of a complete (interpolated) outgoing longwave radiation dataset. *Bulletin of the American Meteorological Society*, 77, 1275–1277.
- Pai, D. S., & Rajeevan, M. (2009). Summer monsoon onset over Kerala: New definition and prediction. *Journal of Earth System Science*, 118(2), 123–135.
- Rasmusson, E. M., & Carpenter, T. H. (1983). The relationship between eastern equatorial Pacific sea surface temperature and rainfall over India and Sri Lanka. *Monthly Weather Review*, 111, 517–528.
- Ropelewski, C. F., & Halpert, M. S. (1987). Global and regional scale precipitation patterns associated with the El Nino/southern oscillation. *Monthly Weather Review*, 115, 1606–1626.
- Ropelewski, C. F., & Halpert, M. S. (1989). Precipitation patterns associated with the high index phase of the southern oscillation. *Journal of Climate*, 2, 268–284.
- Shukla, J. (1987). Interannual variability of monsoon. In J. S. Fein & P. L. Stephens (Eds.), *Monsoons* (pp. 399–464). New York: Wiley.
- Sikka, D. R. (1980). Some aspects of the large-scale fluctuations of summer monsoon rainfall over India in relation to fluctuations in the planetary and regional scale circulation parameters. *Proceedings of the Indian Academy of Sciences (Earth and Planetary Sciences)*, 89, 179–195.
- Wang, B., & LinHo, (2002). Rainy season of the Asian-Pacific summer monsoon. *Journal of Climate*, 15, 386–398.
- Wu, R., & Wang, B. (2001). Multi-stage onset of the summer monsoon over the western North Pacific. *Climate Dynamics*, 17, 277–289.
- Yadav, R. K. (2009a). Changes in the large-scale features associated with the Indian summer monsoon in the recent decades. *International Journal of Climatology*, 29, 117–133.
- Yadav, R. K. (2009b). Role of equatorial central Pacific and northwest of North Atlantic 2-metre surface temperatures in modulating Indian summer monsoon variability. *Climate Dynamics*, 32, 549–563.
- Zhou, L., & Murtugudde, R. (2014). Impact of northward-propagating intraseasonal variability on the onset of Indian summer monsoon. *Journal of Climate*, 27, 126–139.

(Received June 30, 2015, revised May 20, 2016, accepted June 23, 2016, Published online June 28, 2016)

Geoinformatics and Atmospheric Science

Niedzielski, T.; Migala, K. (Eds.)

2018, X, 274 p. 136 illus., 106 illus. in color., Softcover

ISBN: 978-3-319-66091-2

A product of Birkhäuser Basel